

Relaxation of Exciton Confinement in CdSe Quantum Dots by Modification with a Conjugated Dithiocarbamate Ligand

Matthew T. Frederick and Emily A. Weiss*

Department of Chemistry, Northwestern University, 2145 Sheridan Road, Evanston, Illinois 60208

This article describes the use of an organic ligand, phenyldithiocarbamate (PTC), to decrease the energy of the optical band gap, E_g , of colloidal solution-phase CdSe quantum dots (QDs) upon coordination to the surfaces of the QDs. We exposed solutions of a series of QDs with 10 different radii ($R = 1.1 - 1.9$ nm) to PTC, a known chelator of Cd^{2+} ions,^{1,2} and monitored the ground-state absorption and steady-state photoluminescence (PL) spectra of the QDs periodically for up to 6 days as the native ligands (primarily alkylphosphonates and hexadecylamine)³ exchanged for the PTC ligands. These QDs have band-edge absorption maxima that range from 490 to 575 nm when coordinated to their native ligands. During the ligand-exchange process, we observed continuous, parallel shifts of the band-edge absorption, λ_{abs} , and PL peaks, λ_{PL} (Table 1), of the QDs to longer wavelengths. After 6 days, the bathochromic shifts in λ_{abs} ranged from 17 nm ($\Delta E_g = 62$ meV) for the largest QDs to 46 nm ($\Delta E_g = 220$ meV) for the smallest QDs. These values of ΔE_g are the largest shifts achieved by chemical modification of the surfaces of solution-phase CdSe QDs⁴ and are—by more than an order of magnitude in energy—the largest bathochromic shifts achieved for QDs in either the solution or solid phases.^{5,6} Our observed values of ΔE_g correspond to an apparent increase in R of the QDs of 0.26 ± 0.03 nm (approximately the distance from the sulfurs to the nitrogen of PTC), averaged over the entire set of sizes of QDs we studied; this size-independent increase in excitonic radius suggests that PTC shifts E_g by relaxing the quantum confinement of the exciton. Density functional theory (DFT) cal-

ABSTRACT Coordination of phenyldithiocarbamate (PTC) ligands to solution-phase colloidal CdSe quantum dots (QDs) decreases the optical band gap, E_g , of the QDs by up to 220 meV. These values of ΔE_g are the largest shifts achieved by chemical modification of the surfaces of solution-phase CdSe QDs and are—by more than an order of magnitude in energy—the largest bathochromic shifts achieved for QDs in either the solution or solid phases. Measured values of ΔE_g upon coordination to PTC correspond to an apparent increase in the excitonic radius of 0.26 ± 0.03 nm; this excitonic delocalization is independent of the size of the QD for radii, $R = 1.1 - 1.9$ nm. Density functional theory calculations indicate that the highest occupied molecular orbital of PTC is near resonant with that of the QD, and that the two have correct symmetry to exchange electron density (PTC is a π -donor, and the photoexcited QD is a π -acceptor). We therefore propose that the relaxation of exciton confinement occurs through delocalization of the photoexcited hole of the QD into the ligand shell.

KEYWORDS: CdSe quantum dot · quantum confinement · bathochromic shift · dithiocarbamate · ligand exchange

culations suggest that this relaxation occurs through delocalization of the photoexcited hole of the QD into the PTC ligand shell.

RESULTS AND DISCUSSION

Preparation of Phenyldithiocarbamate (PTC)-Coordinated QDs. The Methods section and the Supporting Information contain details of the synthesis of the CdSe QDs and PTC, purification of the QDs, and ligand-exchange procedures. Briefly, to synthesize the CdSe QDs, we added trioctylphosphine oxide (TOPO), hexadecylamine (HDA), and cadmium stearate (CdSt_2) to a dry 50 mL three-neck round-bottom flask and heated the mixture to 320 °C with stirring under positive nitrogen flow. After the CdSt_2 completely dissolved to form an optically clear solution, we rapidly injected trioctylphosphine selenide (TOPSe, 1 mL of 1 M solution in TOP, prepared and stored in a glovebox) and arrested the growth of the QDs by adding 10 mL of room-temperature CHCl_3 directly to the reaction mixture.

*Address correspondence to e-weiss@northwestern.edu.

Received for review April 11, 2010 and accepted May 20, 2010.

Published online May 26, 2010. 10.1021/nn1007435

© 2010 American Chemical Society

TABLE 1. Change in Optical Bandgap, ΔE_g (from Absorbance and PL Measurements) and Apparent Change in Radius, ΔR^a , of CdSe QDs upon Ligand Exchange with PTC for 6 Days

absorbance data				PL data ^a		
$\lambda_{\text{abs},0}$ (nm)	$\Delta\lambda_{\text{abs}}$ (nm)	ΔE_g (from abs) (meV)	ΔR^b (from abs) (nm)	$\lambda_{\text{PL},0}$ (nm)	$\Delta\lambda_{\text{PL}}$ (nm)	ΔE_g (from PL) (meV)
490	46	220	0.27			
504	41	190	0.28			
518	31	140	0.24	529	29	122
536	24	99	0.24	545	24	96
541	24	97	0.26			
554	22	84	0.27	562	20	76
558	20	76	0.27			
563	21	79	0.31			
567	15	56	0.23	575	15	55
575	17	62	0.29			

^aPhotoluminescence measurements were made on randomly selected sizes of QDs. ^bApparent increase in the QD radius, R , corresponding to the observed decrease in E_g .

Cooling immediately after injection of TOPSe resulted in QDs with $R = 1.3$ nm. We produced larger QDs by holding the temperature at 290 °C for longer times. We synthesized the NH_4PTC salt by adding 1 equiv of aniline dropwise to 2 equiv of carbon disulfide in a rapidly stirring suspension of excess concentrated ammonium hydroxide at 0 °C, stirred for 1 h, washed the resulting white powder with CHCl_3 , and dried overnight under vacuum.

We introduced the PTC ligands to the QDs through biphasic ligand exchange with the NH_4PTC salt. We added ~ 4 mg of NH_4PTC —either as a dry, crystalline powder, or, for more accuracy, as 0.24 mL of a freshly prepared 0.1 M aqueous solution of NH_4PTC , which we then allowed to dry completely—to a dry scintillation vial. We added 4 mL of $1.2 \pm 0.2 \mu\text{M}$ QDs in CH_2Cl_2 to the vial, such that the molar ratio of PTC to QDs in the mixture was 5000:1, and stirred the mixture vigorously in the dark. Even after 6 days, the QD–PTC system did not achieve equilibrium because the NH_4PTC is not soluble in CH_2Cl_2 (or any solvent in which the QDs are soluble; see Supporting Information). The biphasic exchange allowed us to separate the QD dispersions from any unreacted NH_4PTC by filtering the contents of the vials with 0.45 μm syringe filters. The unreacted NH_4PTC was a white solid; no colored precipitates deposited on the filters (*i.e.*, the QDs passed completely through the filters). The insolubility of NH_4PTC in CH_2Cl_2 caused the process to take longer than expected for a strong-binding ligand like PTC. The exchange achieves $\sim 95\%$ of saturation within 48 h (Figures 1A and S2); we carried out the process for 6 days, however, in order to ensure that all samples were exchanged to approximately the same degree. Ligand exchange with the sodium salt of PTC (NaPTC), which is soluble in CH_2Cl_2 , was unsuccessful for reasons explained in the Supporting Information. Inductively coupled atomic emission spectroscopy (ICP-AES) indicates that, for QDs with an initial absorption at 558 nm, at the saturation of the bathochromic shift, there is 1 PTC molecule (with two coordinating

sulfur groups) per 10 metal ions on the surface of each QD (see Supporting Information).

Optical Properties of QDs upon Coordination to PTC. Figure 1A shows a representative set of absorption spectra for solutions of CdSe QDs (here, with $R = 1.3$ nm) in CH_2Cl_2 recorded over the first 6 days of ligand exchange with PTC. The value of λ_{abs} shifts from 518 to 540 nm after 19 h and to 549 nm after 6 days; the Supporting Information contains a plot of the time dependence of λ_{abs} . We also measured the PL spectrum of randomly selected sizes of QDs upon exchange with PTC; the PL maximum, λ_{PL} , shifts by approximately the same en-

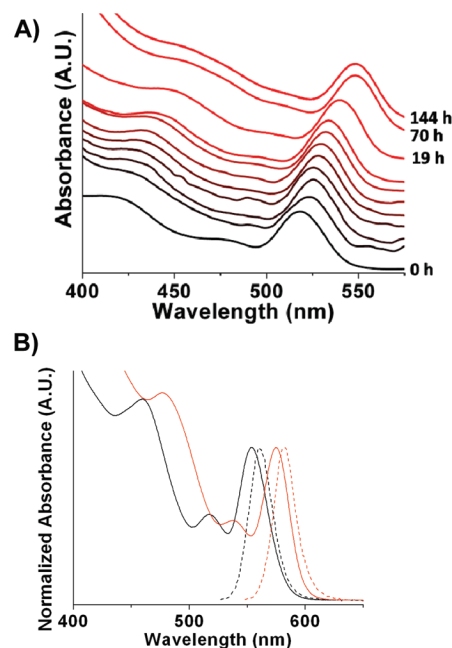


Figure 1. (A) Normalized ground-state absorption spectra (offset along the y-axis) of CdSe QDs in CH_2Cl_2 with $R = 1.3$ nm throughout the first 6 days of exposure to PTC. (B) Absorbance (solid lines) and PL (dashed lines) spectra of QDs with $R = 1.6$ nm before (black) and after (red) exchange with PTC for 6 days. These spectra are representative of the samples we studied in that, upon coordination with PTC, the PL spectra shifted by approximately the same energy as did the absorbance spectra, and neither the absorbance nor PL spectra broadened in energy (see Table S2 in the Supporting Information).

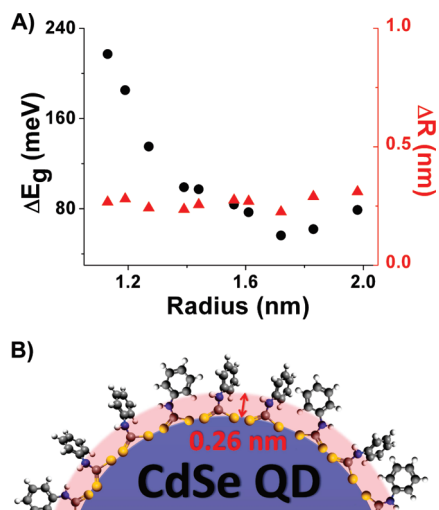


Figure 2. (A) ΔE_g , the decrease in optical band gap (obtained from absorbance measurements) of the QDs after exposure to PTC for 6 days (black, left axis), and ΔR , the apparent change in excitonic radius of the QDs corresponding to the observed values of ΔE_g (red, right axis) plotted against the initial radius, R , of the QDs. (B) Idealized schematic diagram of the proposed delocalization of the excitonic wave function of the QDs due to coordination of PTC. For every size of QD, the observed shift in λ_{abs} corresponds to an increase in the radius, ΔR , of the exciton by 0.26 nm.

ergy as λ_{abs} (Figure 1B and Table 1). Figure 2A shows that the magnitude of ΔE_g (values listed in Table 1) decreases as R increases, but for every size of QD, ΔE_g achieved by functionalizing the QD with PTC corresponds to an apparent increase in the excitonic radius, ΔR , of the QD by the same length: 0.26 ± 0.03 nm.⁷

The effect of PTC on the PL quantum yield varied with size: for $R = 1.6$, the quantum yield decreased from 6.5 to 4.9% upon exchange, but for QDs with $R = 1.1$ and 1.4 nm, exchange with PTC almost completely quenched the PL (see Supporting Information). We suspect this variation in quenching efficiency has less to do with the size of the QD than with overall surface passivation, as well as surface coverage of PTC, but more systematic experiments are needed to clarify this issue.

Probable Mechanism for the Bathochromic Shift Is

Delocalization of the Excitonic Hole into the Ligand Shell. Several mechanisms are proposed in the literature for bathochromic shifts of the optical band gap of semiconductor QDs, including (i) delocalization of the exciton into an inorganic^{8–11} or organic ligand shell upon ligand exchange,^{5,6,10,12} (ii) increase in the average radius of the QDs by, for example, Ostwald ripening in solution,^{13,14} (iii) increase in the dielectric constant of the surrounding medium (solvatochromism),^{10,15} and (iv) coupling of excitons on separate QDs through dipole–dipole interactions¹⁶ or delocalization of an exciton over multiple QDs that are cross-linked or aggregated in solution or films.^{5,6,15}

The dependence of ΔE_g on the size of QDs exposed to NH_4PTC (Figure 2A and Table 1), which shows that the apparent change in excitonic radius, ΔR , is constant

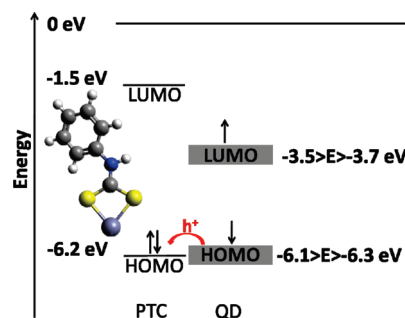


Figure 3. Diagram showing the energetic alignment of the HOMOs of QDs used in this study (with $R = 1.1–1.9$ nm) with that of the HOMO of Cd^{2+} –PTC (structure shown in its optimized geometry, where sulfurs are in yellow, nitrogen is in blue, carbons are in dark gray, and the Cd^{2+} ion is in light gray), as calculated by DFT using a 6-311G** basis set and an LANL2DZ effective core potential for Cd^{2+} . The Supporting Information contains orbital density maps for the HOMO through HOMO-3 of Cd^{2+} –PTC.

with R provides the most compelling evidence that PTC acts through mechanism (i), stabilization of the excitonic state of the QD through delocalization of the exciton—or, more specifically, delocalization of either the photoexcited electron or hole wave function—into the ligand shell, shown schematically in Figure 2B. We cannot say definitively where the “edge” of the exciton is for QDs functionalized with their native ligands, but the delocalization radius of 0.26 nm is comparable to the experimentally measured Cd–S bond length (0.26 nm) within Cd^{2+} –diethyldithiocarbamate complexes in solution^{1,2} and to the distance between the sulfurs and nitrogen of PTC (0.20 nm), assuming the geometry-optimized gas-phase structure of PTC chelated to Cd^{2+} (DFT, B3LYP, 6-311G** with LANL2DZ effective core potential for Cd^{2+}) (Figure 3, inset).

Density functional theory calculations suggest that the mechanism by which coordination to PTC decreases the confinement energy of the excitonic state is through delocalization of the wave function of the excitonic hole into the ligand shell. The geometry-optimized PTC-chelated Cd^{2+} molecule (see Supporting Information) has a HOMO with $E_{\text{HOMO}} = -6.24$ eV relative to vacuum (Figure 3). This orbital, which extends over the entire PTC molecule, including the CS_2 headgroup, is within 0.1 eV of the energy of the HOMOs (valence band edges) of the QDs that we studied ($R = 1.1–1.9$ nm), as predicted by the effective mass approximation^{17,18} (Figure 3). We believe that this energetic resonance and spatial coupling leads to mixing of the HOMOs of the QD with those of PTC. These orbitals are also of the correct symmetry to mix: the HOMOs of the QD are composed primarily of Se 4p orbitals¹⁹ and, when half-filled (in the excited state), act as π -acceptors. The HOMOs of the Cd^{2+} –PTC complex (HOMO through HOMO-3) are predominately composed of the p-orbitals of sulfur, carbon, and nitrogen and act as π -donors (see Supporting Information for orbital density maps). In the first few (energetically tightly packed) exci-

tonic states of the QD, this orbital mixing enables a partial transfer of the hole into the HOMO of the ligand shell, which allows delocalization of the confined exciton wave function and subsequent energetic stabilization of the first few excited states of the QD, as manifested in the bathochromic shift of the corresponding transitions in the absorption and PL spectra (Figure 1).

This mechanism for relaxation of exciton confinement has been seen previously. For example, dithiocarbamates shift the electrochemical potentials of bulk CdSe by donating electron density to surface states.²⁰ Previous work has shown that coordination of CN⁻ ligands to CdSe QDs produces hypsochromic shifts of ~300 meV.⁴ We believe that the CN⁻ ligands shift the energy of the exciton by a mechanism analogous to that of PTC, except that, while PTC is π -donor, CN⁻ is a π -acceptor (it supports π -backbonding). The PTC ligands therefore accept hole density from the valence band of the QDs (delocalizing the hole wave function and stabilizing the exciton), while CN⁻ ligands donate hole density (confining the hole wave function and destabilizing the exciton).

In order to investigate the chemical features of PTC that enable it to induce relaxation of quantum confinement of the exciton, we compared the value of ΔE_g achieved after 6 days of ligand exchange with PTC to that achieved with the same molar ratio of benzylmercaptan (BzM), the thiol analogue of PTC, for QDs with $R = 1.4$ nm. While both of these ligands produced bathochromic shifts of the band-edge absorption peak, PTC ($\Delta E_g = 99$ meV) is much more effective than BzM ($\Delta E_g = 10$ meV). This result shows that the presence of a sulfur-containing headgroup or a conjugated core is not sufficient to produce our observed shifts. Furthermore, previous measurements showed that, upon coordination to CdSe QDs, secondary and aliphatic dithiocarbamates produce either no shift²¹ or a hypsochromic shift of the optical band gap,²² probably due to corrosion of the QDs, as we observed when we exposed the QDs to *n*-octyldithiocarbamate (see Supporting Information). We believe, therefore, that the delocalization of the exciton into the ligand shell is facilitated by both strong bidentate^{1,2} binding of the CS₂ headgroup to Cd²⁺ on the surface of the QDs—which allows for strong spatial coupling of the orbitals of the ligand to orbitals of the core—and the conjugation of sulfur atoms of the headgroup with the nitrogen.

Other Mechanisms for a Bathochromic Shift of the QD Absorption Spectrum—Growth of QDs, Aggregation of QDs, and Solvatochromism—Are Inconsistent with Experimental Observations. Previous work indicates that Ostwald ripening of CdSe QDs (mechanism ii) does not occur at temperatures below 240 °C without addition of Cd and Se precursors.^{11,13,14} In addition, growth of QDs leads to an increase in size dispersity and PL line width and, in some cases, splitting of absorption peaks.^{7,13,14} We observe that the excitonic radius of every size of QD in-

creases by the same $\Delta R = 0.26$ nm, whereas ΔR induced by Ostwald ripening is greater for initially smaller QDs than for larger QDs such that the system minimizes the total interfacial free energy. Furthermore, we observe no increase in the line widths of PL or band-edge absorption peaks upon ligand exchange with PTC (Table S2 in the Supporting Information). In fact, we consistently see a *decrease* in the absorption and PL line widths by between 10% and 25%. This narrowing of optical spectra—particularly the absorption line width since it cannot be narrowed by energy transfer or a decrease in the emitting population—is consistent with the mechanism of relaxation of quantum confinement inducing the bathochromic shift, because smaller QDs within an ensemble will experience larger shifts in λ_{abs} and λ_{PL} than will larger QDs. The Supporting Information contains a comparison of simulated line widths (assuming the exciton delocalization mechanism) and actual line widths of PL spectra of several samples of QDs. The ability of our proposed mechanism to predict the observed narrowing of absorbance and PL spectra is strong evidence that this mechanism is responsible for the bathochromic shift.

Unfortunately, we cannot acquire meaningful statistics on the size of PTC-exchanged QDs from TEM analysis because we have observed that the PTC-exchanged QDs are not stable to the combination of high vacuum and heating by the electron beam in the microscope. This structural instability, which we believe is a result of tighter binding of Cd²⁺ on the surface to PTC than to the Se²⁻ in the QD lattice, results in migration of surface Cd²⁺ and manifests in the images as fused QDs and nonspherical shapes of QDs. In some instances, we can see the “melting” phenomena occur over time in the TEM (see Supporting Information). The QDs with their native ligands probably do not undergo this melting because their long-chain alkyl ligands are tightly packed on the surface—and therefore stabilized by intermolecular interactions—and bind more weakly to the Cd²⁺ than does Se²⁻, so the Cd²⁺ cannot migrate. The Supporting Information shows images of samples pre-PTC exchange and post-PTC exchange (for 6 days) where we could identify individual QDs and the average and standard deviation of R for each individual image; on the basis of these limited statistics, the difference in the sizes before and after exchange is within the uncertainty of the measurement.

Although the dielectric environment of the ligand shell changes when PTC replaces the aliphatic native ligands, we do not believe that mechanism (iii), solvatochromism, is responsible for ΔE_g because the predicted magnitude of the solvatochromic effect is between 5 and 14 times smaller than what we observe for PTC exchange. For example, a change in local dielectric constant, ϵ , from 2.1 to 6.2 (equivalent to going from a hexanes solution of QDs to a solid film of QDs) produces only a 10 meV shift in E_g .¹⁵ We observed no change in ΔE_g upon changing the dielectric environment of the

QDs from solution in CH_2Cl_2 to a dried film (deposited postexchange with PTC; see Supporting Information). Additionally, no apparent solvatochromic effect is present in samples of QDs coordinated to various para-substituted aniline compounds, which have higher dielectric constants ($\epsilon = 7.2$) than do the aliphatic native ligands ($\epsilon = 2.1$),²³ or in samples of QDs coordinated to CN^- ligands ($\epsilon = 7.6$), which actually produce a strong *hypsochromic* shift of the absorption spectra, as discussed in the previous section.⁴

Finally, we believe that the bathochromic shift is not due to the QDs' cross-linking or aggregating (mechanism iv) because (1) the solutions of QDs after PTC exchange are optically clear ($\text{OD} < 0.01$ at wavelengths longer than those of the first absorption peak) and pass completely through submicrometer filters, after which their absorption spectra are identical to those prefiltering; (2) the value of ΔE_g that we observe is up to 14 times larger than that predicted and observed for aggregation of CdSe QDs of similar radius in close-packed films;¹⁵ and (3) the full-width-at-half-maximum of the PL peak decreases after exposure of the QDs to PTC (Table S2). The decreased line width of the PL peak indicates that exchange with PTC induces neither energy transfer among the QDs nor an increase in the dispersity in R within the ensemble.⁷

CONCLUSIONS

The surfactant-induced stabilization of the exciton in CdSe QDs through delocalization of the wave function of one of the excitonic charge carriers has several important potential implications: (i) *Facilitation of fundamental electrochemical characterization of QDs.* We believe that functionalization of QDs with PTC (or ligands with similar chemical structure) will increase the stability of QDs to electrochemical processes by replacing the insulating ligand shell—which collects charge until dielectric breakdown produces unstable QDs vulnerable to rapid decomposition²⁴—with a conductive ligand shell that more effectively couples the QD core to its surrounding medium. The ability to

oxidize and reduce the QD core would then facilitate quantitative measurements of electrochemical potentials of QDs and thereby aid in the design of QD/(organic,QD,semiconductor) heterojunctions for charge separation in solar cells or photocatalytic devices. (ii) *Increased tunability of the excitonic radius.* Although several methodologies exist for size-focusing synthesis and purification of QDs, we have shown that the ligand shell provides an additional “knob” to turn in determining the excitonic radius of the QD. We are currently exploring the effects of para-substituted phenyldithiocarbamates on E_g of CdSe QDs because we hypothesize that adjusting the electron density on the nitrogen and the geometry of the N- CS_2 group will provide an additional degree of tunability for the radius and energy of the QD exciton. (iii) *Increased electronic coupling for energy-transfer-mediated logic switching.* QD–molecule hybrids are ideal materials for highly nondissipative logic switching because they can transmit signals through energy transfer (which involves less vibrational reorganization and therefore less energy lost as heat than does charge transfer) and because the large frequency contrast between the bonds in the QD (between heavy metals) and those in the molecule (between light organics) inhibits dissipation through vibrational energy redistribution. Exciton-delocalizing ligands such as PTC will maximize the electronic coupling for, and therefore the rate and yield of, long-range energy transfer within QD–molecule films for this application. (iv) *Increased robustness and electrical conductivity of QD-based optoelectronic devices.* Solid-state devices such as photovoltaic cells, transistors, and light-emitting diodes require strong electronic coupling of QDs to each other and to their surroundings in order to conduct charge efficiently and undergo quick reproducible cycles of charging and discharging. Wessels *et al.*²⁵ have shown that films of gold nanoparticles cross-linked by conjugated dithiocarbamates show a 10^6 -fold increase in conductivity over those with alkanethiols; we believe a similar effect will be possible with QD–dithiocarbamate-based devices.

METHODS

Synthesis and Purification of CdSe Quantum Dots. We used all reagents and solvents, including trioctylphosphine oxide (TOPO, 90%), trioctylphosphine (TOP, 90%), selenium shot, hexadecylamine (HDA), hexanes, and methanol, as-received from Sigma Aldrich, except cadmium stearate, which we used as-received from MP Biomedicals, Inc. We added TOPO (1.94 g, 5.02 mmol), HDA (1.94 g, 8.03 mmol), and cadmium stearate (0.112 g, 0.165 mmol) to a dry 50 mL three-neck round-bottom flask and heated the mixture to 320 °C with stirring under positive nitrogen flow. After the cadmium stearate completely dissolved to form an optically clear solution, we rapidly injected trioctylphosphine selenide (TOPSe, 1 mL of 1 M solution in TOP, prepared and stored in a glovebox). We arrested the growth of the QDs by quenching the reaction with 10 mL of chloroform after allowing the solution to cool to 220 °C. Cooling the entire reaction mixture immediately after injection

of TOPSe resulted in QDs with $\lambda_{\text{abs}} = 518$ nm ($R = 1.3$ nm). We produced larger QDs ($R = 1.6$ and 1.7 nm) by holding the temperature at 290 °C for longer times. Quantum dots with $\lambda_{\text{abs}} = 490, 504, 541, 563, 575,$ and 582 nm ($R = 1.1, 1.2, 1.4, 1.7, 1.8,$ and 1.9 nm) were produced from one reaction mixture by taking aliquots at approximately 1 min intervals and quenching immediately in 1.5 mL of CHCl_3 . Once the reaction mixture (or aliquots thereof) cooled to room temperature, we added 20 mL of methanol and centrifuged the mixture (at 3500 rpm for 5 min) to precipitate the QDs. We dispersed the resulting pellet in 10 mL of hexanes and centrifuged again. We collected the supernatant and allowed it to sit for 24 h in the dark, during which time a white precipitate (excess cadmium stearate, TOPO, and HDA) formed. Centrifugation of this suspension produced a white pellet of free ligand, which we discarded, and a colored supernatant that contained the QDs. We dried the QD solution under nitrogen stream and dispersed in CH_2Cl_2 .

Synthesis of Ammonium Phenylthiocarbamate (NH₄PTC). Following the procedure of Wessels *et al.*²⁵ with slight modifications, we added 5 mL of aniline dropwise over 15 min to 1.5 equiv of carbon disulfide (CS₂) in 30 mL of concentrated ammonium hydroxide at 0 °C under nitrogen atmosphere and stirred the solution for 30 min. During this time, the solution turned red. The light yellow product, ammonium phenylthiocarbamate (NH₄PTC), precipitated from solution (see Supporting Information for an absorbance spectrum). We suction-filtered the product, washed with 30 mL of CHCl₃, and dried under vacuum. The yield of the pure product by ¹³C and ¹H NMR was 37%: ¹H NMR (500 MHz, D₂O) δ 7.29 (m, 4H, H_{arom}), 7.18 (m, 1H, H_{arom}); ¹³C NMR (500 MHz, D₂O) δ 213.73 (–NH–CS₂), 140.54 (C–NH–CS₂), 128.91, 126.85, 126.09 (C_{arom} × 3).²⁶

DFT Calculations. The geometry optimizations and orbital energy calculations were performed with QChem 3.1²⁷ software using a LANL2DZ effective core potential for Cd²⁺ with the matching basis set of 6-311G** and B3LYP functional.

Acknowledgment. This work was supported by the Non-equilibrium Energy Research Center (NERC), which is an Energy Frontier Research Center funded by the U.S. Department of Energy, Office of Science, Office of Basic Energy Sciences under Award Number DE-SC0000989. The authors thank Carmen Herrmann, Gemma Solomon, and Alex Weckiewicz for their help in performing the DFT calculations, and Brian Rolczynski and Lin Chen for assistance in TCSPC experiments. The TEM work was performed in the EPIC facility of NUANCE Center at Northwestern University. NUANCE Center is supported by NSF-NSEC, NSF-MRSEC, Keck Foundation, the State of Illinois, and Northwestern University.

Supporting Information Available: Additional experimental methods, TEM images and additional ground state absorption spectra of the QDs, ICP-AES measurements of surface coverage of PTC, time-resolved PL and PL quantum yield measurements, results of molecular orbital calculations, Figures S1–S11, and Tables S1, S2. This material is available free of charge via the Internet at <http://pubs.acs.org>.

REFERENCES AND NOTES

- Erenburg, S. B.; Bausk, N. V.; Zemskova, S. M.; Mazalov, L. N. Spatial Structure of Transition Metal Complexes in Solution Determined by EXAFS Spectroscopy. *Nucl. Instrum. Methods* **2000**, *448*, 345–350.
- Mazalov, L. N.; Bausk, N. V.; Erenburg, S. B.; Larionov, S. V. X-ray Investigation of the Structure of Metal Chelate Dithiocarbamate Complexes in Solution. *J. Struct. Chem.* **2001**, *42*, 784–793.
- Morris-Cohen, A. J.; Donakowski, M. D.; Knowles, K. E.; Weiss, E. A. The Effect of a Common Purification Procedure on the Chemical Composition of the Surfaces of CdSe Quantum Dots Synthesized with Trioctylphosphine Oxide. *J. Phys. Chem. C* **2009**, *114*, 897–906.
- Sarkar, S. K.; Chandrasekharan, N.; Gorer, S.; Hodes, G. Reversible Adsorption-Enhanced Quantum Confinement in Semiconductor Quantum Dots. *Appl. Phys. Lett.* **2002**, *81*, 5045–5047.
- Koole, R.; Liljeroth, P.; de Mello Donega, C.; Vanmaekelbergh, D.; Meijerink, A. Electronic Coupling and Exciton Energy Transfer in CdTe Quantum-Dot Molecules. *J. Am. Chem. Soc.* **2006**, *128*, 10436–10441.
- Koole, R.; Luijckx, B.; Tachiya, M.; Pool, R.; Vlugt, T. J. H.; de Mello Donega, C.; Meijerink, A.; Vanmaekelbergh, D. Differences in Cross-Link Chemistry between Rigid and Flexible Dithiol Molecules Revealed by Optical Studies of CdTe Quantum Dots. *J. Phys. Chem. C* **2007**, *111*, 11208–11215.
- Yu, W. W.; Qu, L.; Guo, W.; Peng, X. Experimental Determination of the Extinction Coefficient of CdTe, CdSe, and CdS Nanocrystals. *Chem. Mater.* **2003**, *15*, 2854–2860.
- Jin, T.; Fujii, F.; Yamada, E.; Nodasaka, Y.; Kinjo, M. Control of the Optical Properties of Quantum Dots by Surface Coating with Calix[n]Arene Carboxylic Acids. *J. Am. Chem. Soc.* **2006**, *128*, 9288–9289.
- Tsay, J. M.; Doose, S.; Pinaud, F.; Weiss, S. Enhancing the Photoluminescence of Peptide-Coated Nanocrystals with Shell Composition and UV Irradiation. *J. Phys. Chem. B* **2005**, *109*, 1669–1674.
- Algar, W. R.; Krull, U. J. Luminescence and Stability of Aqueous Thioalkyl Acid Capped CdSe/ZnS Quantum Dots Correlated to Ligand Ionization. *ChemPhysChem* **2007**, *8*, 561–568.
- Dorfs, D.; Franzl, T.; Osovsky, R.; Brumer, M.; Lifshitz, E.; Klar, T. A.; Eychmüller, A. Type-I and Type-II Nanoscale Heterostructures Based on CdTe Nanocrystals: A Comparative Study. *Small* **2008**, *4*, 1148–1152.
- Thuy, U. T. D.; Liem, N. Q.; Thanh, D. X.; Protière, M.; Reiss, P. Optical Transitions in Polarized CdSe, CdSe/ZnSe, and CdSe/CdS/ZnS Quantum Dots Dispersed in Various Polar Solvents. *Appl. Phys. Lett.* **2008**, *91*, 241908–241911.
- Li, R.; Luo, Z.; Papadimitrakopoulos, F. Redox-Assisted Asymmetric Ostwald Ripening of CdSe Dots to Rods. *J. Am. Chem. Soc.* **2006**, *128*, 6280–6281.
- Sung, Y.-M.; Park, K.-S.; Lee, Y.-J.; Kim, T.-G. Ripening Kinetics of CdSe/ZnSe Core/Shell Nanocrystals. *J. Phys. Chem. C* **2006**, *111*, 1239–1242.
- Leatherdale, C. A.; Bawendi, M. G. Observation of Solvatochromism in CdSe Colloidal Quantum Dots. *Phys. Rev. B* **2001**, *63*, 165315/1–165315/6.
- Boev, V. I.; Filonovich, S. A.; Vasilevskiy, M. I.; Silva, C. J.; Gomes, M. J. M.; Talapin, D. V.; Rogach, A. L. Dipole–Dipole Interaction Effect on the Optical Response of Quantum Dot Ensembles. *Physica B* **2003**, *338*, 347–352.
- Norris, D. J.; Bawendi, M. G. Measurement and Assignment of the Size-Dependent Optical Spectrum in CdSe Quantum Dots. *Phys. Rev. B* **1996**, *53*, 16338–16346.
- Van de Walle, C. G.; Neugebauer, J. Universal Alignment of Hydrogen Levels in Semiconductors, Insulators and Solutions. *Nature* **2003**, *423*, 626–628.
- Albe, V.; Jouanin, C.; Bertho, D. Confinement and Shape Effects on the Optical Spectra of Small CdSe Nanocrystals. *Phys. Rev. B* **1998**, *58*, 4713–4720.
- Thackeray, J. W.; Natan, M. J.; Ng, P.; Wrighton, M. S. Interaction of Diethyldithiocarbamate with n-Type Cadmium Sulfide and Cadmium Selenide: Efficient Photoelectrochemical Oxidation to the Disulfide and Flat-Band Potential of the Semiconductor as a Function of Adsorbate Concentration. *J. Am. Chem. Soc.* **1986**, *108*, 3570–3577.
- Wang, J.; Xu, J.; Goodman, M. D.; Chen, Y.; Cai, M.; Shinar, J.; Lin, Z. A Simple Biphasic Route to Water Soluble Dithiocarbamate Functionalized Quantum Dots. *J. Mater. Chem.* **2008**, *18*, 3270–3274.
- Liu, D.; Wu, W.; Qiu, Y.; Lu, J.; Yang, S. Chemical Conjugation of Fullerene C₆₀ to CdSe Nanocrystals via Dithiocarbamate Ligands. *J. Phys. Chem. C* **2007**, *111*, 17713–17719.
- Knowles, K. E.; Tice, D. B.; McArthur, E. A.; Solomon, G. C.; Weiss, E. A. Chemical Control of the Photoluminescence of CdSe Quantum Dot–Organic Complexes with a Series of Para-Substituted Aniline Ligands. *J. Am. Chem. Soc.* **2009**, *132*, 1041–1050.
- Haram, S. K.; Quinn, B. M.; Bard, A. J. Electrochemistry of CdS Nanoparticles: A Correlation between Optical and Electrochemical Band Gaps. *J. Am. Chem. Soc.* **2001**, *123*, 8860–8861.
- Wessels, J. M.; Nothofer, H.-G.; Ford, W. E.; von Wrochem, F.; Scholz, F.; Vossmeier, T.; Schroedter, A.; Weller, H.; Yasuda, A. Optical and Electrical Properties of Three-Dimensional Interlinked Gold Nanoparticle Assemblies. *J. Am. Chem. Soc.* **2004**, *126*, 3349–3356.
- Humeres, E.; Debacher, N. A.; Franco, J. D.; Lee, B. S.; Martendal, A. Mechanisms of Acid Decomposition of Dithiocarbamates. 3. Aryldithiocarbamates and the Torsional Effect. *J. Org. Chem.* **2002**, *67*, 3662–3667.
- Shao, Y.; *et al.* Advances in Methods and Algorithms in a Modern Quantum Chemistry Program Package. *Phys. Chem. Chem. Phys.* **2006**, *8*, 3172–3191.